Evidence for an EPR-Detectable Semiquinone Intermediate Stabilized in the Membrane-Bound Subunit NarI of Nitrate Reductase A (NarGHI) from *Escherichia coli*†

Stéphane Grimaldi,*,‡ Pascal Lanciano,‡ Patrick Bertrand,‡ Francis Blasco,§ and Bruno Guigliarelli‡

Unité de Bioénergétique et Ingénierie des Protéines (UPR9036) and Laboratoire de Chimie Bactérienne (UPR9043), Institut de Biologie Structurale et de Microbiologie, CNRS, and Université de Provence, 31 Chemin Joseph Aiguier, 13402 Marseille Cedex 20, France

Received September 15, 2004; Revised Manuscript Received November 10, 2004

ABSTRACT: Nitrate reductase A (NRA, NarGHI) is expressed in *Escherichia coli* by growing the bacterium in anaerobic conditions in the presence of nitrate. This enzyme reduces nitrate to nitrite and uses menaquinol (or ubiquinol) as the electron donor. The location of quinones in the enzyme, their number, and their role in the electron transfer mechanism are still controversial. In this work, we have investigated the spectroscopic and thermodynamic properties of a semiquinone (SQ) in membrane samples of overexpressed *E. coli* nitrate reductase poised in appropriate redox conditions. This semiquinone is highly stabilized with respect to free semiquinone. The *g*-values determined from the numerical simulation of its Q-band (35 GHz) EPR spectrum are equal to 2.0061, 2.0051, 2.0023. The midpoint potential of the Q/QH_2 couple is about −100 mV, and the SQ stability constant is about 100 at pH 7.5. The semiquinone EPR signal disappears completely upon addition of the quinol binding site inhibitor 2-*n*-nonyl-4-hydroxyquinoline *N*-oxide (NQNO). A semiquinone radical could also be stabilized in preparations where only the NarI membrane subunit is overexpressed in the absence of the NarGH catalytic dimer. Its thermodynamic and spectroscopic properties show only slight variations with those of the wild-type enzyme. The X-band continuous wave (cw) electron nuclear double resonance (ENDOR) spectra of the radicals display similar proton hyperfine coupling patterns in NarGHI and in NarI, showing that they arise from the same semiquinone species bound to a single site located in the NarI membrane subunit. These results are discussed with regard to the location and the potential function of quinones in the enzyme.

Nitrate reductase A (NarGHI)[1] is the dominant respiratory complex in *Escherichia coli* when the bacterium is grown under anaerobic conditions in the presence of nitrate (for recent review, see ref *1*). This complex catalyzes nitrate reduction in the cytoplasm and couples the transfer of electrons from quinol to nitrate to the release of protons into the periplasm, which generates a transmembrane proton electrochemical potential (*2*). The heterotrimeric NarGHI complex is composed of (i) a catalytic subunit (NarG, 139 kDa) containing a Mo-bisMGD cofactor and a [4Fe-4S] cluster (FS0), (ii) an electron transfer subunit (NarH, 58 kDa) carrying one [3Fe-4S] cluster (FS4) and three [4Fe-4S] clusters (FS1 to FS3 according to their distance to the Mo cofactor), and (iii) a membrane anchor subunit (NarI, 26 kDa) containing two *b*-type hemes (b_D and b_P). The latter subunit mediates the transfer of electrons from the quinone pool of the membrane to the molybdenum cofactor. NarGHI is able to use either menaquinol (MQH_2) or ubiquinol (UQH_2) as physiological reductants (*3*). The protons generated by the oxidation of MQH_2 are released into the periplasm during enzyme turnover so that the proton translocation stoichiometry is thought to be $2H^+/2e^-$ (*2*, *4*).

The coordination and redox properties of hemes b_P and b_D and of the iron−sulfur clusters have been extensively studied by optical and EPR spectroscopies in combination with mutagenesis studies and redox potentiometry (*1*): the low-potential (b_D, +20 mV) and high-potential (b_P, +120 mV) hemes were shown to be located near the periplasmic side and the cytoplasmic side of the membrane, respectively (*5*). The iron−sulfur centers of NarH have been classified into two classes with markedly different redox potentials (*6*, *7*): the high-potential group comprises the [3Fe-4S] cluster FS4 (+180 mV) and FS1 (+130 mV). FS2 (−420 mV) and FS3 (−55 mV) belong to the low-potential group (*8*−*10*). These studies allowed us to determine the coordinating cysteine residues of these clusters and to propose a model for their organization within the protein (*1*). The recently solved X-ray crystal structures of the whole enzyme NarGHI (*11*) and of the soluble complex NarGH (*12*) have confirmed

† This work was supported by the CNRS and the Université de Provence.

* Corresponding author: fax, (+00 33) 491164578; phone, (+00 33) 491164557; e-mail, grimaldi@ibsm.cnrs-mrs.fr.

‡ Unité de Bioénergétique et Ingénierie des Protéines.

§ Laboratoire de Chimie Bactérienne.

[1] Abbreviations: A_1, phylloquinone in photosystem I; cw, continuous wave; ENDOR, electron nuclear double resonance spectroscopy; EPR, electron paramagnetic resonance spectroscopy; HQNO, 2-heptyl-4-hydroxyquinoline *N*-oxide; MQ, menaquinone; MQH_2, menaquinol; NarGHI, *Escherichia coli* nitrate reductase A; NarI(ΔGH), *E. coli* nitrate reductase A lacking the soluble complex NarGH; NQNO, 2-nonyl-4-hydroxyquinoline *N*-oxide; NRA, nitrate reductase A; Q-site, quinone binding site; Q_A and Q_B, primary and secondary stable electron acceptors in type II reaction centers; Q_H, high-affinity ubiquinone binding site of cytochrome *bo*; Q_P, quinone oxidation site of nitrate reductase; SQ, semiquinone radical anion.

10.1021/bi048009r CCC: $30.25
Published on Web 12/31/2004

these findings. They have moreover provided a detailed picture of the overall architecture of the complex as well as new information such as the presence of a previously undetected FeS cluster (FS0) in the NarG subunit and the unique coordination of the Mo atom by an Asp side chain. The structure shows that the eight redox cofactors are organized in a linear way, suggesting that electron transfer takes place through a unique chain within the enzyme. However, the alternation of high- and low-potential FeS clusters along this chain casts doubts on its efficiency. Indeed, the remarkably broad range over which the FeS redox potentials are spread (~600 mV) and the significant activities displayed by mutated enzymes where a high-potential cluster was selectively removed (*7*, *13*) raise questions about the role of the FeS clusters.

In contrast with metal centers, little is known about the number, the location, and the role of quinones which are the NRA physiological partners. A first indication about the presence of intrinsic quinones in NarGHI came from a work on the extraction and purification of NarGH, which suggested the presence of a tightly bound (nondissociable) menaquinone-9 which is copurified with the NarGH catalytic dimer (*14*). In a subsequent study, a transient 2-heptyl-4-hydroxyquinoline *N*-oxide (HQNO) sensitive radical signal detected by EPR spectroscopy in two NarH mutants of NarGHI lacking the iron−sulfur cluster FS1 ($NarGH^{C16A}I$ and $NarGH^{C263A}I$) was attributed to a SQ radical (*15*). During enzyme turnover, following the addition of nitrate to dithionite-reduced membranes containing overexpressed NRA, the decrease of the radical signal intensity was followed by the appearance of the $[3Fe\text{-}4S]^{1+}$ EPR signal, suggesting that the radical species is located before the [3Fe-4S] cluster in the electron transfer pathway to nitrate. This species was proposed to be the anionic semiquinone form of the menaquinone previously identified in NarGH (*15*). Since this radical could not be detected in the wild-type enzyme, its observation in both mutants was explained by a decrease of the electron transfer rate within NarGHI consecutive to the loss of FS1.

Using quinol analogue substrates and inhibitors in combination with optical, fluorescence, and EPR spectroscopies (*16*, *17*), it was shown that both HQNO and stigmatellin are strong inhibitors of the quinol:nitrate oxidoreductase activity (*16*). HQNO binding appears to occur at a single site and strongly affects the spectroscopic and thermodynamic properties of heme b_D (*16*, *17*). On the basis of these data, a model for quinol binding was proposed in which a single high-affinity site (the Q_P site) is located toward the periplasmic side of NarI in close proximity to heme b_D. Quinol binding and oxidation by NarGHI have also been addressed by several steady-state enzymatic studies. However, the conclusions about the number and the nature of the quinone binding sites are different: when the menaquinol analogues reduced lapachol and plumbagin were used as substrates, the observed kinetics were consistent with the binding to a single site within the NarGHI complex (*18*, *19*). However, a more detailed analysis using menaquinol and ubiquinol analogues suggested the presence of two quinol binding sites, one for ubiquinol and the other for menaquinol (*20*, *21*). Recently, stopped-flow experiments detected a transient species by measuring absorbance changes at 390 nm (corresponding to the maximum absorption of the menadione radical anion) after mixing NarGHI membranes with menadiol, a menaquinol analogue used as an electron donor (*22*, *23*). This transient species was assigned to a menadione radical anion associated with the enzyme. This study was interpreted in terms of a second menaquinone binding site in the enzyme. In the recently solved X-ray structure of NarGHI, an elongated hydrophobic cavity exposing both hemes to the lipid bilayer was proposed as a potential binding site for one or two quinones (*11*). However, no quinone could be modeled in the electron density map. Therefore, the number, the location, and the role of quinones are still controversial in NarGHI.

In membrane proteins of the respiratory chains, the stabilization of the intermediate semiquinone state is an obligatory step in the catalytic cycle of the enzymes. Electron paramagnetic resonance (EPR) spectroscopy has already been used to detect several semiquinone radical species in mutant or wild-type enzymes of *E. coli* respiratory chains, such as quinol:fumarate reductase (QFR) (*24*) and cytochromes *bd* (*25*) and *bo* (*26*, *27*). For the latter, the use of more advanced EPR methods such as higher frequency EPR (*28*−*30*) or electron nuclear double resonance (ENDOR) spectroscopies (*28*, *30*) has proven to be useful to gain further insights into the binding of the high-affinity semiquinone Q_H to the protein.

In this work, we report the detection and the characterization by EPR spectroscopy of a thermodynamically stabilized semiquinone in *E. coli* membrane preparations containing overexpressed wild-type NRA. A semiquinone species is also observed in membrane preparations where only the NarI subunit is overexpresssed. ENDOR experiments carried out on these radicals in NarGHI and NarI(ΔGH) demonstrate that they arise from the same species bound to a single site.

MATERIALS AND METHODS

Bacterial Strain and Plasmids. E. coli JCB20480, a *napA*::*ery* derivative of LCB2048, was used as the host for all of the experiments described herein (*31*). NarGHI was expressed from plasmid pVA700, which encodes the entire NarGHI operon (*7*). Plasmid pCD7 was used to express a NarI(ΔGH) mutant (*7*, *15*).

Growth Conditions and Preparation of Membrane Fractions. Cells were grown semianaerobically in 2.5 L Erlenmeyer flasks containing Terrific Broth medium at 35 °C and pH 7.0 according to the method described in ref *9*. Enzyme overexpression was induced with 0.2 mM isopropyl 1-thio-β-D-galactopyranoside (IPTG). When appropriate, ampicillin (100 μg mL^{-1}), spectinomycin (50 μg mL^{-1}), and kanamycin (50 μg mL^{-1}) were included in the growth medium. JCB20480 membranes lacking NarGHI were prepared by the same method as above except that ampicillin and IPTG were not used in the growth medium. Cells were harvested and washed, and membranes were prepared by French pressure cell lysis and differential centrifugation (*32*). Membrane vesicles were suspended in 100 mM MOPS− 5 mM EDTA at pH 7.5.

Membrane preparations were assayed for protein concentration by the method of Lowry et al. (*33*), modified as previously described (*15*). Rocket immunoelectrophoresis was carried out as described in ref *34*. After concentration of membrane preparations, the total protein content was estimated to be in the 50−130 mg/mL range, depending on preparations. According to the level of protein overexpression

(~20%), this corresponds to NRA concentrations in the 40−120 μM range.

Redox Titration Experiments. Redox titrations were performed at room temperature (about 25 °C) in an airtight vessel flushed with oxygen-free argon. Redox potentials were measured with a combined Pt-Ag/AgCl/KCl (3 M) microelectrode as described in ref *6* and are given in the text with respect to the standard hydrogen electrode. The following redox mediators were used at 10 μM final concentrations: dichloroindophenol (+217 mV), 1,2-naphthoquinone (+145 mV), phenazine ethosulfate (+55 mV), methylene blue (+11 mV), resorufine (−51 mV), indigocarmine (−125 mV), and phenosafranine (−252 mV). Reductive titrations were carried out by stepwise addition of an anaerobic sodium dithionite solution (100 mM), and samples were transferred anaerobically into calibrated EPR tubes which were frozen and stored in liquid nitrogen. The variation of the normalized semiquinone EPR signal amplitude (*A*) was fitted to a theoretical curve corresponding to two successive one-electron redox processes:

$$A = 1/\{1 + \exp[(E - E_1)F/RT] + \exp[(E_2 - E)F/RT]\} \quad (1)$$

where E_1 and E_2 are the midpoint potentials of the Q/SQ and SQ/QH_2 couples, respectively, *R* and *F* are the molar gas and Faraday constants, respectively, and *T* is absolute temperature. The midpoint potential of the Q/QH_2 couple, which corresponds to the maximal amount of semiquinone, is $E_m = (E_1 + E_2)/2$. The stability constant K_s of SQ defined with respect to the disproportionation reaction is

$$K_s = [SQ]^2/[Q][QH_2] = \exp[(E_1 - E_2)F/RT] \quad (2)$$

EPR and ENDOR Spectroscopies. All EPR measurements were performed on a Bruker Elexsys E500 spectrometer. X-band EPR spectra were recorded using a standard rectangular Bruker EPR cavity fitted to an Oxford Instruments helium flow cryostat (ESR900). Q-band EPR spectra were measured using a standard Bruker resonator (ER 5106QT) equipped with an Oxford Instruments CF 935 cryostat. For *g*-value measurements, the microwave frequency was measured by using a Hewlett-Packard HP1552B frequency counter, and magnetic field values were corrected against a known *g*-standard (weak pitch, $g = 2.0028 \pm 0.0001$). The simulation of powder spectra was carried out using a Matlab program (The MathWorks, Inc., Natick, MA) described in ref *35*. The powder spectrum given by a disordered frozen solution is obtained by summation over approximately 1000 orientations uniformly distributed on a half-sphere. To account for inhomogeneous broadening effects, the spectrum is then convoluted with an isotropic Gaussian line.

^{1}H-ENDOR spectra were recorded using a Bruker DICE extension, a 250 W radio-frequency amplifier from Amplifier Research, and a Bruker EN 801 cw-ENDOR resonator. They are presented in the first-derivative mode. The radio-frequency wave was modulated at 25 kHz with a modulation depth of 200 kHz. For isotropic ENDOR spectra of weakly coupled protons, each coupled proton is expected to give rise to two lines which are symmetrically spaced with respect to the proton nuclear Larmor frequency ν_H and separated by the proton hyperfine coupling constant, *A*. The ENDOR frequencies, ν_{ENDOR}, are therefore given by $\nu^{\pm}_{ENDOR} = \nu_H \pm A/2$ (*36*).

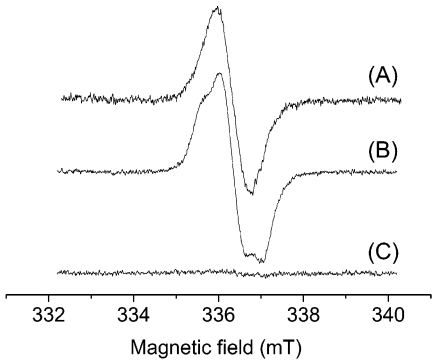

FIGURE 1: X-band EPR spectra of stabilized radicals in dithionite-reduced *E. coli* membranes (JCB20480). The samples were poised at the potential leading to the maximum SQ signal, which was deduced from the titration curves at pH 7.5. (A) Wild-type NarGHI-enriched membranes (JCB20480/pVA700), $E = -90$ mV. (B) Membranes containing NarI(ΔGH) overexpressed from the pCD7 plasmid, $E = -13$ mV. (C) JCB20480 membranes, $E = -87$ mV. Spectra were recorded under the following conditions: temperature, 60 K; microwave power, 10 μW; modulation amplitude, 0.3 mT; modulation frequency, 100 kHz; microwave frequency, 9.425 GHz.

RESULTS

Stabilization of a Semiquinone Radical in NarGHI Overexpressed in E. coli Membranes. To investigate whether transient semiquinone radicals can be observed in wild-type nitrate reductase, *E. coli* membranes enriched in NarGHI complexes were prepared and reduced in the absence of substrate by addition of sodium dithionite in excess. The reduction was performed directly in an EPR tube which was frozen after 2 min incubation. The EPR spectra of this sample recorded at 60 K revealed an intense isotropic radical signal centered at $g \sim 2.0045$ with a peak-to-peak line width of about 0.8 mT (not shown). This signal was strongly attenuated when the experiment was repeated in the presence of NQNO (500 μM) (not shown). This behavior and the spectral properties strongly suggest that this radical signal arises from a semiquinone species.

To further study the thermodynamic stability of the observed radical, a redox titration followed by EPR of a membrane preparation buffered at pH 7.5 was carried out between +400 and −400 mV. A radical signal was observed in the 0 to −200 mV range with a maximum amplitude at about −100 mV (Figure 1). No change of the signal shape was observed in this potential range. The variation of the signal amplitude displayed the bell shape expected for quinone species undergoing a reduction in two successive one-electron transfer steps (Figure 2). The same behavior was observed with different membrane preparations. When the data were fitted with theoretical curves based on eq 1, midpoint potential values equal to $E_1 = -40 \pm 10$ mV and $E_2 = -150 \pm 10$ mV were obtained, giving $E_m = -95$ mV and a SQ stability constant $K_s \approx 70$.

To check that the radical species is located in the NarGHI complex, similar titration experiments were carried out on membrane fractions from *E. coli* strain JCB20480 devoid of NRA. No significant radical signal could be detected in the whole potential range (Figure 1C). Titration experiments

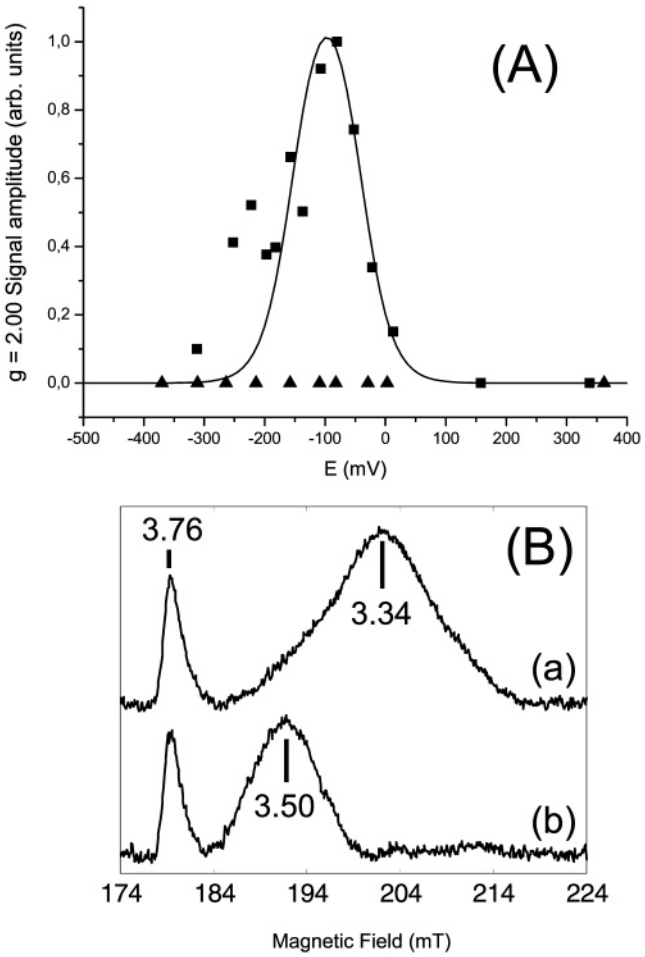

FIGURE 2: (A) Potentiometric titration curves of the SQ radical in NarGHI in the absence (■) and in the presence (▲) of 500 μM NQNO. The peak-to-peak amplitude measured at $g \approx 2$ is plotted as a function of the ambient potential. The solid line is the theoretical curve calculated from eq 1 with $E_1 = -40$ mV and $E_2 = -150$ mV. EPR experiments were conducted as described in the legend of Figure 1. (B) Effect of NQNO on the low-spin heme EPR spectrum of NarGHI in *E. coli* membranes. Spectra are (a) without inhibitor and (b) in the presence of 500 μM NQNO. The spectra were obtained by accumulating nine scans; a polynomial baseline correction was applied to the experimental spectrum in order to remove the background signal arising from the free iron signal at $g \sim 4.3$. Spectra were recorded at 12.5 K with a microwave power of 20 mW and a field modulation of 1 mT at 100 kHz.

were also performed on *E. coli* NarGHI-enriched membranes in the presence of the menaquinone analogue NQNO, an efficient quinone binding site inhibitor of respiratory membrane proteins. Binding of the inhibitor to the oxidized enzyme was manifested by a characteristic shift of the g_z peak of heme b_D from 3.34 to 3.50, which is similar to that observed in the enzyme with bound HQNO at the Q_P site (*16*) (Figure 2B). In these conditions, no radical signal could be detected by EPR in the whole potential range (Figure 2A). This provides strong support in favor of the semiquinonic nature of the detected radical species.

To measure the semiquinone occupancy level in NarGHI, the spin intensity corresponding to the maximal SQ signal was determined by double integration of the EPR spectrum recorded in nonsaturating conditions (60 K, 10 μW). This intensity was compared to that given by the $[3Fe\text{-}4S]^{1+}$ center in an oxidized sample of the same membrane preparation. The maximum concentration of the semiquinone species was

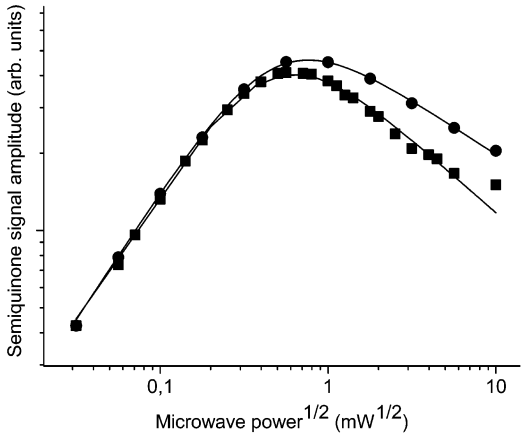

FIGURE 3: Power saturation profile of the semiquinone signals recorded at 150 K in NarGHI-enriched membranes (■) and in NarI-(ΔGH)-enriched membranes (●) poised at $E = -90$ and -13 mV, respectively (pH 7.5). The data were analyzed by computer fitting to the empirical equation $I = A\sqrt{P}/(1 + P/P_{1/2})^{b/2}$, where I is the peak-to-peak intensity of the EPR signal, P is the microwave power, $P_{1/2}$ is the half-saturation microwave power, b is the "inhomogeneity parameter", and A is a normalization constant. The best fits shown as solid lines were obtained by using $P_{1/2} = 0.22$ mW and $b = 1.57$ for NarGHI and $P_{1/2} = 0.25$ mW and $b = 1.43$ for NarI-(ΔGH). arb. units = arbitrary units.

estimated to be 0.27 ± 0.05 SQ/[3Fe-4S] cluster at pH 7.5, which indicates that a SQ radical is present in about 30% of NRA enzymes. In addition, the saturation behavior of the radical signal was studied at 150 K. To facilitate the comparison with other studies carried out on protein-bound semiquinones, the data were fitted with a curve calculated from an empirical equation (*37*). The $P_{1/2}$ value of 0.22 mW deduced from the fit (Figure 3) is typical of slow relaxing semiquinone species (*24*).

Stabilization of a Semiquinone Radical in NarI(ΔGH) Overexpressed in E. coli Membranes. To specify the location of the radical within NRA, similar experiments were carried out on *E. coli* membranes enriched only in the NarI subunit. As in the case of the wild-type enzyme, a radical species could be detected by EPR, either trapped by reduction with dithionite and freezing or stabilized during a redox titration. In both cases, the EPR intensity was found to be comparable to that given by the radical observed in the wild-type enzyme. Although the positions of the two signals are very similar ($g \sim 2.0045$), the signal given by the NarI(ΔGH) subunit exhibits a composite shape (Figure 1B) which could arise from a conformational heterogeneity of the radical. Alternatively, it could come from partially resolved splittings due either to hyperfine coupling to closely associated nuclear spins or to spin−spin interactions with another paramagnetic center. The results of a potentiometric redox titration of the radical signal in NarI(ΔGH) are shown in Figure 4. No change of the signal shape was observed in the +100 to −200 mV potential range and in the 12−200 K temperature range. The signal titrates according to a bell-shaped curve which is slightly shifted toward higher redox potentials by comparison with that observed in the case of NarGHI. Curve-fitting computer analysis provided $E_1 = -8 \pm 10$ mV and $E_2 = -110 \pm 10$ mV, which corresponds to $E_m = -59$ mV and $K_s \sim 50$. The saturation profile of the SQ signal recorded at 150 K is shown in Figure 3. The data could be fitted to a single saturation curve characterized by a $P_{1/2}$ value equal

Table 1: *g*-Tensor Principal Values of Membrane Protein-Bound Semiquinone Radicals As Determined by EPR Spectroscopy

	E. coli nitrate reductase A, menaSQ[a,i]	*E. coli* cytochrome *bo*, ubiSQ Q_H[b]	spinach photosystem II, plastoSQ Q_A[c]	*Rb. sphaeroides* reaction center		spinach photosystem I, phylloSQ A_1[f,g]	*Rps. viridis* reaction center, menaSQ Q_A[h]
				ubiSQ Q_A[d]	ubiSQ Q_B[e]		
g_x	2.0061	2.00593	2.00661	2.0066	2.00626	2.00609	2.00597
g_y	2.0051	2.00543	2.00506	2.0054	2.00527	2.00503	2.00492
g_z	2.0023	2.00220	2.00215	2.0022	2.00210	2.00210	2.00216
g_{iso}	2.0045	2.00452	2.0046	2.0047	2.00455	2.00441	2.00435

[a] This work. [b] From ref *30*. [c] From ref *52*. [d] From ref *53*. [e] From ref *54*. [f] From ref *55*. [g] From ref *56*. [h] From ref *57*. [i] Abbreviations: MenaSQ, menasemiquinone; ubiSQ, ubisemiquinone; plastoSQ, plastosemiquinone; phylloSQ, phyllosemiquinone; $g_{iso} = (1/3)(g_x + g_y + g_z)$; *Rb.*, *Rhodobacter*; *Rps.*, *Rhodopseudomonas*.

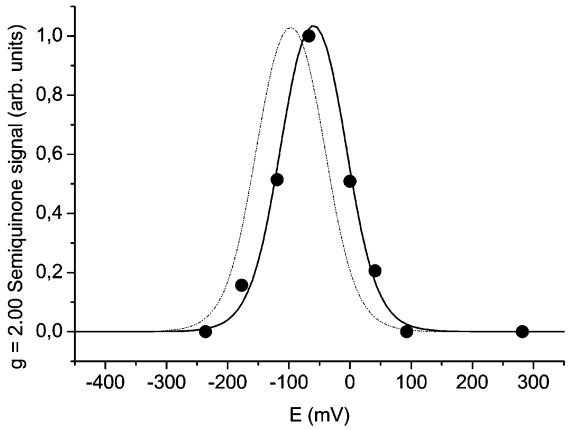

FIGURE 4: Potentiometric titration curve of the $g \approx 2.00$ semiquinone signal in NarI(ΔGH)-enriched membranes. Experimental data were fitted as described in Materials and Methods using $E_1 = -8$ mV and $E_2 = -110$ mV. Experimental conditions were as described in the legend of Figure 1. The fit of the titration curve of the radical in NarGHI is recalled as dotted lines for comparison.

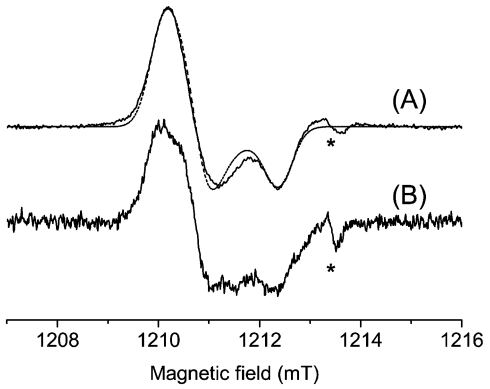

FIGURE 5: Q-band EPR spectra of the semiquinone species in overexpressed (A) NarGHI (JCB20480/pVA700) and (B) NarI(ΔGH) (JCB20480/pCD7). Membranes were redox poised at −90 mV (A) and −22 mV (B). Experimental conditions: temperature, 80 K; microwave power, 0.5 μW; microwave frequency, 33.9776 GHz (A) and 34.0021 GHz (B); modulation amplitude, 0.5 mT; modulation frequency, 100 kHz. A numerical simulation of the NarGHI spectrum, shown as dotted lines, was obtained with $g_x = 2.0061$, $g_y = 2.0051$, $g_z = 2.0023$ (±0.0001), and an isotropic Gaussian line width of 0.38 mT. Signals indicated by asterisks are due to impurities in the Q-band cavity.

to 0.25 mW (Figure 3), which is a value very similar to that obtained for the SQ in NarGHI.

Q-Band (35 GHz) EPR Characterization of Semiquinones in NarGHI and NarI(ΔGH). X-band EPR experiments performed on NarGHI and NarI yield only the average *g*-value of the radical signals. To resolve the *g*-tensor principal values, higher frequency EPR measurements were carried out. The Q-band EPR spectrum of NarGHI in *E. coli* membranes at 90 K is shown in Figure 5. The sample was poised at the potential value where the amount of SQ is maximum (−90 mV). The spectrum exhibits the characteristic axial line shape expected for a single semiquinone species with $g_\perp = 2.0055$ (measured at the zero crossing of the EPR line) and $g_\parallel = 2.0023$ (high-field minimum of the first derivative). The *g*-tensor principal values deduced from the numerical simulation of the spectrum are $g_x = 2.0061$, $g_y = 2.0051$, and $g_z = 2.0023$ (±0.0001). An isotropic Gaussian line with a 0.38 mT width was used to account for unresolved hyperfine splittings. The *g*-values are very similar to those reported for semiquinones observed in other respiratory systems (Table 1), which confirms the semiquinonic nature of the radicals detected in nitrate reductase. Q-band measurements were also performed on *E. coli* membranes containing overexpressed NarI(ΔGH). The Q-band EPR spectrum of the sample poised at a redox potential where the SQ signal is maximum is depicted in Figure 5. The overall anisotropy of the *g*-tensor is similar to that observed in the case of NarGHI, but as at X-band, additional features can be observed in the spectrum. This indicates that the NarI(ΔGH) spectrum is composed of a main component, identical to that given by NarGHI, and of a minor species exhibiting partially resolved structures.

X-Band Continuous Wave ENDOR Spectroscopy of Semiquinones in NarGHI and NarI(ΔGH). To detect hyperfine couplings between the semiquinones and the surrounding magnetic nuclei, ENDOR experiments were carried out on *E. coli* membrane fractions enriched in either NarGHI or NarI complexes. The samples were prepared at the redox potential where the amount of SQ is maximum, and ENDOR experiments were performed at different temperatures in the 20−120 K range. At each temperature, the microwave and radio-frequency powers were optimized so as to get the maximum ENDOR signal. ENDOR spectra obtained at 80 K from overexpressed NarGHI-containing membranes (A) and overexpressed NarI(ΔGH)-containing membranes (B) are shown in Figure 6. They were recorded with the static magnetic field value set at the center of the radical EPR spectrum. Due to the relatively low enzyme concentration in the membrane fractions (typically 50 μM) and to the intrinsically low sensitivity of the ENDOR technique, it was necessary to accumulate the spectra during several hours to achieve an acceptable signal-to-noise ratio. The dominant spectral feature appears around 14 MHz, which is the ^{1}H Larmor frequency in the experimental conditions used. It arises from weakly coupled protons located in the vicinity of the SQ species, the so-called matrix protons (*38*). Other ENDOR features symmetrically positioned with respect to

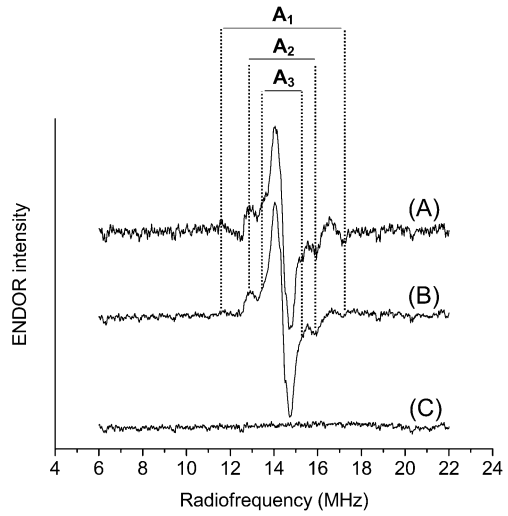

FIGURE 6: ^{1}H-ENDOR spectra of (A) NarGHI-enriched membranes (−90 mV) and (B, C) NarI(ΔGH)-enriched membranes (−13 mV). In (A) and (B), the magnetic field was set at the maximum of the EPR spectrum [(A) 338.20 mT and (B) 337.96 mT]. In (C), it was set outside the EPR signal (335.89 mT). Other experimental conditions were as follows: temperature, 80 K; microwave frequency, 9.478 GHz; microwave power, 5 mW; radio-frequency power, 110 W; time constant and conversion time, 20.48 ms; number of scans, 1680 (A), 552 (B), and 490 (C).

the ^{1}H Larmor frequency could be identified, corresponding to hyperfine couplings equal to $A_1 = 5.7$ MHz, $A_2 = 3.3$ MHz, and $A_3 = 1.8$ MHz. These resonances were not observed when the static magnetic field value was set outside the SQ EPR spectrum (Figure 6C). Previous ENDOR studies of semiquinone radicals in membrane-bound proteins have shown that couplings of this magnitude come from protons which are more strongly coupled to the radical, such as those involved in hydrogen bonding to the quinone or those belonging to the quinone ring (*28*, *39*−*42*). The magnitude of these couplings is strongly dependent on the electronic structure of the semiquinone and of its close environment. Interestingly, the ENDOR spectra given by the NarGHI and NarI(ΔGH) preparations display the same proton ENDOR line shapes and hyperfine coupling values (Figure 6A,B). This demonstrates that the same semiquinone radical is responsible for the NarGHI spectrum and for the major spectral component of NarI. ENDOR resonances associated with the minor spectral component found in the NarI(ΔGH) EPR spectrum could not be detected, presumably because of the low sensitivity of cw-ENDOR.

DISCUSSION

In this study, we have demonstrated that a SQ radical species can be thermodynamically stabilized in membrane-bound NarGHI overexpressed in *E. coli*. By working on NarGHI-enriched membranes, one avoids possible alterations of the thermodynamic and spectroscopic properties of the prosthetic groups which could result from the extraction of the protein from the membranes. Moreover, overexpression facilitates the specific detection of prosthetic groups belonging to NarGHI complex.

The characteristics of the EPR spectrum displayed at X-band by the radical species in NarGHI (e.g., isotropic line centered at $g \sim 2.0045$ with a 0.8 mT line width) and its saturation properties are very similar to those reported for membrane-bound semiquinone radicals in respiratory systems such as the bc_1 complex (*43*−*46*), NADH dehydrogenase (*47*, *48*), cytochromes *bo* (*26*, *27*) and *bd* (*25*), and quinol:fumarate reductase (*24*). Moreover, the *g*-values deduced from the numerical simulation of Q-band spectra are also very similar to those obtained with other protein-bound semiquinones (Table 1). This allows an unambiguous assignment of the radical detected in NarGHI to a semiquinone species, which is also supported by the sensitivity of the spectrum to the NQNO quinone analogue. Besides, the Q-band measurements and the saturation data strongly suggest that a single semiquinone species contributes to the EPR spectrum.

Our results reveal that the binding of quinone to the nitrate reductase complex induces a strong stabilization of the SQ form. Indeed, the stability constant ($K_s \sim 70$) of the radical in NarGHI is even larger than that of the high-affinity Q_H ubisemiquinone in cytochrome *bo* (*26*, *27*) and appears to be several orders of magnitude larger than the K_s of the semiquinone radical observed in a mutant of quinol:fumarate reductase from *E. coli* (*24*). This indicates that the semiquinone is tightly bound to its binding site in NarGHI.

A strong EPR signal arising from a semiquinone radical could also be generated and stabilized in NarI(ΔGH)-enriched membranes. The EPR and redox properties of this SQ were found to differ slightly from those observed in NarGHI. In NarI(ΔGH), the midpoint potential of the Q/QH_2 couple is shifted at higher potential by about 40 mV, and the stability constant of SQ is slightly decreased to $K_s \sim 50$. Moreover, the EPR signal of SQ in NarI(ΔGH) displays additional features which could arise either from spectral heterogeneity or from different interactions with other magnetic species. It is worth noting that the E_m values of heme b_P drops from +120 mV in NarGHI to −178 mV in NarI(ΔGH) (*17*) so that the SQ and heme b_P can be simultaneously paramagnetic in NarI(ΔGH). However, the peculiar shape of the SQ signal is not modified when the temperature is raised from 12 to 200 K, which demonstrates that the additional spectral features are not due to the spin−spin coupling between SQ and heme b_P. This is confirmed by the fact that the relaxation properties of the SQ species are essentially the same in NarI(ΔGH) and NarGHI (Figure 3). Moreover, the $P_{1/2}$ value is much smaller than that measured for the fast relaxing SQ species detected in quinol:fumarate reductase, which is likely coupled to a $[3Fe\text{-}4S]^{1+}$ cluster by spin−spin interactions (*24*). The peculiar shape of the SQ EPR signal in NarI(ΔGH) could arise from different hyperfine interactions with one or several nuclei of the binding pocket. However, ENDOR experiments performed on SQ in NarGHI and NarI(ΔGH) preparations gave essentially identical spectra with dominant hyperfine coupling constants $A_1 = 5.7$ MHz, $A_2 = 3.3$ MHz, and $A_3 = 1.8$ MHz. Such values are typical of methyl group protons of the semiquinone and of protons involved in hydrogen bonding to the oxygen atom of the quinone. For instance, the methyl protons were found to give a strong ENDOR signal at cryogenic temperatures, characterized by an approximately axial hyperfine coupling tensor (*38*, *49*). The values of the two components, $A_\perp$ and $A_{||}$, of this tensor are 4 and 7.1 MHz and 4.7 and 7.9 MHz for Q_A^- and Q_B^- in the reaction center from *Rhodobacter sphaeroides*, respectively (*39*, *50*), and reach 9.7 and 13.3 MHz for Q_H^- in cytochrome *bo* from *E. coli* (*28*, *30*). Moreover, exchangeable

protons assigned to H-bond with hyperfine coupling constants equal to 4.7 and 6.5 MHz for Q_A^- and 3.1 and 5.1 MHz for Q_B^- have been detected in the *Rb. sphaeroides* reaction center. In the case of cytochrome *bo* from *E. coli*, coupling constants equal to 2.1, 5.2, and 10.4 MHz have been measured for Q_H (*28*, *51*).

No other hyperfine coupling could be detected in the 10−25 MHz range in the ENDOR spectra of NarI(ΔGH) preparations. Thus, the peculiar line shape of the SQ EPR signal in NarI(ΔGH) likely arises from an additional minor component resulting from some conformational heterogeneity consecutive to the loss of the NarGH complex. In such preparations, the environment of the radical could be slightly modified and the exposure of the semiquinone to the solvent could increase, leading to changes of the redox potentials (Figure 4). It should be pointed out, however, that these spectral and thermodynamic differences are much smaller than those observed for heme b_P whose spectroscopic and thermodynamic properties are dramatically altered in NarI(ΔGH) by comparison with that of the holoenzyme, with a 300 mV decrease of the redox potential and a shift of the g_z-value from 3.76 to 2.92 (*17*). While the properties of heme b_D are only weakly affected by the removal of the NarGH complex, the sensitivity of heme b_P properties is consistent with the crystallographic data which reveal that the C-terminal tail of NarI is inserted into NarH and interacts with NarG (*11*).

The close similarity between the ENDOR spectra, the Q-band spectra, and the redox properties of SQ in NarGHI and NarI(ΔGH) shows clearly that the semiquinone intermediate is stabilized within the same binding site in both preparations. Therefore, the SQ binding site is located within the NarI membrane anchor subunit. In agreement with the X-ray crystal structure of NarGHI and NarGH complexes (*11*, *12*) our results argue against the hypothesis of a nonexchangeable menaquinone bound to the NarGH complex proposed previously (*14*, *15*), although the presence of a menaquinone with no stable semiquinone state cannot be completely excluded. If one considers its spectroscopic properties and its sensitivity to HQNO, it is likely that the radical observed in the course of the reoxidation of the $NarGH^{C16A}I$ mutant lacking the FS1 [4Fe-4S] cluster (*15*) corresponds to a SQ bound to the same Q-site as that discovered in the present study. It is now clear that this SQ radical can be thermodynamically stabilized without loss of any prosthetic group and that it is located in NarI.

The absence of any effect due to the spin−spin interactions between the SQ species and heme b_P in NarI(ΔGH) suggests that the Q-site is rather distant from heme b_P. As HQNO (and thus NQNO as well) binds in the menaquinol oxidation site Q_P, in the vicinity of heme b_D, it is likely that the stabilized SQ we have observed is in Q_P. However, we cannot completely exclude that the NQNO effect is to prevent the reduction of quinone to SQ and that the SQ could be bound to a Q-site distinct from Q_P.

Further spectroscopic experiments combined with site-directed mutagenesis and more detailed analysis of SQ hyperfine interactions are in progress to better specify the binding site and the role of SQ in the catalytic cycle of NRA.

In summary, this is the first report on the direct observation and stabilization of a semiquinone species in wild-type NarGHI overexpressed in *E. coli* membranes. We found that the radical is sensitive to NQNO and that it is highly stabilized in a Q-site located within the NarI membrane subunit.

ACKNOWLEDGMENT

S.G. thanks Prof. T. F. Prisner (University of Frankfurt, Germany) for the use of his EPR simulation program. Dr. W. Nitschke (BIP-CNRS, Marseille) is acknowledged for the kind gift of NQNO. We are indebted to Dr. G. Roger (BIP-CNRS, Marseille) for his essential assistance during the EPR and ENDOR experiments.

REFERENCES

1. Blasco, F., Guigliarelli, B., Magalon, A., Asso, M., Giordano, G., and Rothery, R. A. (2001) The coordination and function of the redox centres of the membrane-bound nitrate reductases, *Cell. Mol. Life Sci. 58*, 179−193.
2. Jones, R. W., Lamont, A., and Garland, P. B. (1980) The mechanism of proton translocation driven by the respiratory nitrate reductase complex of *Escherichia coli*, *Biochem. J. 190*, 79−94.
3. Wallace, B. J., and Young, I. G. (1977) Role of quinones in electron transport to oxygen and nitrate in *Escherichia coli*. Studies with a ubiA-menA-double quinone mutant, *Biochim. Biophys. Acta 461*, 84−100.
4. Berks, B. C., Page, M. D., Richardson, D. J., Reilly, A., Cavill, A., Outen, F., and Ferguson, S. J. (1995) Sequence analysis of subunits of the membrane-bound nitrate reductase from a denitrifying bacterium: the integral membrane subunit provides a prototype for the dihaem electron-carrying arm of a redox loop, *Mol. Microbiol. 15*, 319−331.
5. Magalon, A., Lemesle-Meunier, D., Rothery, R. A., Frixon, C., Weiner, J. H., and Blasco, F. (1997) Heme axial ligation by the highly conserved His residues in helix II of cytochrome *b* (NarI) of *Escherichia coli* nitrate reductase A, *J. Biol. Chem. 272*, 25652−25658.
6. Guigliarelli, B., Asso, M., More, C., Augier, V., Blasco, F., Pommier, J., Giordano, G., and Bertrand, P. (1992) EPR and redox characterization of iron−sulfur centers in nitrate reductases A and Z from *Escherichia coli*: evidence for a high potential and low potential class and their relevance in the electron transfert mechanism, *Eur. J. Biochem. 207*, 61−68.
7. Guigliarelli, B., Magalon, A., Asso, M., Bertrand, P., Frixon, C., Giordano, G., and Blasco, F. (1996) Complete coordination of the four Fe−S centers of the beta subunit from *Escherichia coli* nitrate reductase. Physiological, biochemical, and EPR characterization of site-directed mutants lacking the highest or lowest potential [4Fe-4S] clusters, *Biochemistry 35*, 4828−4836.
8. Rothery, R. A., Magalon, A., Giordano, G., Guigliarelli, B., Blasco, F., and Weiner, J. H. (1998) The molybdenum cofactor of *Escherichia coli* nitrate reductase A (NarGHI). Effect of a mobAB mutation and interactions with [Fe-S] clusters, *J. Biol. Chem. 273*, 7462−7469.
9. Rothery, R. A., Blasco, F., and Weiner, J. H. (2001) Electron transfer from heme b_L to the [3Fe-4S] cluster of *Escherichia coli* nitrate reductase A (NarGHI), *Biochemistry 40*, 5260−5268.
10. Magalon, A., Asso, M., Guigliarelli, B., Rothery, R. A., Bertrand, P., Giordano, G., and Blasco, F. (1998) Molybdenum cofactor properties and [Fe−S] cluster coordination in *Escherichia coli* nitrate reductase A: investigation by site-directed mutagenesis of the conserved His-50 residue in the NarG subunit, *Biochemistry 37*, 7363−7370.
11. Bertero, M. G., Rothery, R. A., Palak, M., Hou, C., Lim, D., Blasco, F., Weiner, J. H., and Strynadka, N. C. (2003) Insights into the respiratory electron transfer pathway from the structure of nitrate reductase A, *Nat. Struct. Biol. 10*, 681−687.
12. Jormakka, M., Richardson, D., Byrne, B., and Iwata, S. (2004) Architecture of NarGH reveals a structural classification of MobisMGD enzymes, *Structure (Cambridge) 12*, 95−104.
13. Augier, V., Asso, M., Guigliarelli, B., More, C., Bertrand, P., Santini, C. L., Blasco, F., Chippaux, M., and Giordano, G. (1993) Removal of the high-potential [4Fe-4S] center of the beta-subunit from *Escherichia coli* nitrate reductase. Physiological, biochemical, and EPR characterization of site-directed mutated enzymes, *Biochemistry 32*, 5099−5108.

14. Brito, F., DeMoss, J. A., and Dubourdieu, M. (1995) Isolation and identification of menaquinone-9 from purified nitrate reductase of *Escherichia coli*, *J. Bacteriol. 177*, 3728−3735.
15. Magalon, A., Rothery, R. A., Giordano, G., Blasco, F., and Weiner, J. H. (1997) Characterization by electron paramagnetic resonance of the role of the *Escherichia coli* nitrate reductase (NarGHI) iron−sulfur clusters in electron transfer to nitrate and identification of a semiquinone radical intermediate, *J. Bacteriol. 179*, 5037−5045.
16. Magalon, A., Rothery, R. A., Lemesle-Meunier, D., Frixon, C., Weiner, J. H., and Blasco, F. (1998) Inhibitor binding within the NarI subunit (cytochrome *bnr*) of *Escherichia coli* nitrate reductase A, *J. Biol. Chem. 273*, 10851−10856.
17. Rothery, R. A., Blasco, F., Magalon, A., Asso, M., and Weiner, J. H. (1999) The hemes of *Escherichia coli* nitrate reductase A (NarGHI): potentiometric effects of inhibitor binding to narI, *Biochemistry 38*, 12747−12757.
18. Rothery, R. A., Chatterjee, I., Kiema, G., McDermott, M. T., and Weiner, J. H. (1998) Hydroxylated naphthoquinones as substrates for *Escherichia coli* anaerobic reductases, *Biochem. J. 332*, 35−41.
19. Morpeth, F. F., and Boxer, D. H. (1985) Kinetic analysis of respiratory nitrate reductase from *Escherichia coli* K12, *Biochemistry 24*, 40−46.
20. Giordani, R., Buc, J., Cornish-Bowden, A., and Cardenas, M. L. (1997) Kinetics of membrane-bound nitrate reductase A from *Escherichia coli* with analogues of physiological electron donors—different reaction sites for menadiol and duroquinol, *Eur. J. Biochem. 250*, 567−577.
21. Giordani, R., and Buc, J. (2004) Evidence for two different electron transfer pathways in the same enzyme, nitrate reductase A from *Escherichia coli*, *Eur. J. Biochem. 271*, 2400−2407.
22. Zhao, Z., Rothery, R. A., and Weiner, J. H. (2003) Transient kinetic studies of heme reduction in *Escherichia coli* nitrate reductase A (NarGHI) by menaquinol, *Biochemistry 42*, 5403−5413.
23. Zhao, Z., Rothery, R. A., and Weiner, J. H. (2003) Effects of site-directed mutations on heme reduction in *Escherichia coli* nitrate reductase A by menaquinol: a stopped-flow study, *Biochemistry 42*, 14225−14233.
24. Hagerhall, C., Magnitsky, S., Sled, V. D., Schroder, I., Gunsalus, R. P., Cecchini, G., and Ohnishi, T. (1999) An *Escherichia coli* mutant quinol:fumarate reductase contains an EPR-detectable semiquinone stabilized at the proximal quinone-binding site, *J. Biol. Chem. 274*, 26157−26164.
25. Hastings, S. F., Kaysser, T. M., Jiang, F., Salerno, J. C., Gennis, R. B., and Ingledew, W. J. (1998) Identification of a stable semiquinone intermediate in the purified and membrane bound ubiquinol oxidase-cytochrome *bd* from *Escherichia coli*, *Eur. J. Biochem. 255*, 317−323.
26. Ingledew, W. J., Ohnishi, T., and Salerno, J. C. (1995) Studies on a stabilisation of ubisemiquinone by *Escherichia coli* quinol oxidase, cytochrome *bo*, *Eur. J. Biochem. 227*, 903−908.
27. Sato-Watanabe, M., Itoh, S., Mogi, T., Matsuura, K., Miyoshi, H., and Anraku, Y. (1995) Stabilization of a semiquinone radical at the high-affinity quinone-binding site (Q_H) of the *Escherichia coli bo*-type ubiquinol oxidase, *FEBS Lett. 374*, 265−269.
28. Veselov, A. V., Osborne, J. P., Gennis, R. B., and Scholes, C. P. (2000) Q-band ENDOR (electron nuclear double resonance) of the high-affinity ubisemiquinone center in cytochrome bo_3 from *Escherichia coli*, *Biochemistry 39*, 3169−3175.
29. Grimaldi, S., MacMillan, F., Ostermann, T., Ludwig, B., Michel, H., and Prisner, T. (2001) Q_H^- ubisemiquinone radical in the bo_3-type ubiquinol oxidase studied by pulsed electron paramagnetic resonance and hyperfine sublevel correlation spectroscopy, *Biochemistry 40*, 1037−1043.
30. Grimaldi, S., Ostermann, T., Weiden, N., Mogi, T., Miyoshi, H., Ludwig, B., Michel, H., Prisner, T. F., and MacMillan, F. (2003) Asymmetric binding of the high-affinity Q(H)(*)(−) ubisemiquinone in quinol oxidase (bo_3) from *Escherichia coli* studied by multifrequency electron paramagnetic resonance spectroscopy, *Biochemistry 42*, 5632−5639.
31. Potter, L. C., Millington, P. D., Thomas, G. H., Rothery, R. A., Giordano, G., and Cole, J. A. (2000) Novel growth characteristics and high rates of nitrate reduction of an *Escherichia coli* strain, LCB2048, that expresses only a periplasmic nitrate reductase, *FEMS Microbiol. Lett. 185*, 51−57.
32. Rothery, R. A., and Weiner, J. H. (1991) Alteration of the iron−sulfur cluster composition of *Escherichia coli* dimethyl sulfoxide reductase by site-directed mutagenesis, *Biochemistry 30*, 8296−8305.
33. Lowry, O. H., Rosebrough, N. J., Farr, A. L., and Randall, R. J. (1951) Protein measurement with the Folin phenol reagent, *J. Biol. Chem. 193*, 265−275.
34. Augier, V., Guigliarelli, B., Asso, M., Bertrand, P., Frixon, C., Giordano, G., Chippaux, M., and Blasco, F. (1993) Site-directed mutagenesis of conserved cysteine residues within the beta subunit of *Escherichia coli* nitrate reductase. Physiological, biochemical, and EPR characterization of the mutated enzymes, *Biochemistry 32*, 2013−2023.
35. Prisner, T., Lyubenova, S., Atabay, Y., MacMillan, F., Kroger, A., and Klimmek, O. (2003) Multifrequency cw-EPR investigation of the catalytic molybdenum cofactor of polysulfide reductase from *Wolinella succinogenes*, *J. Biol. Inorg. Chem. 8*, 419−426.
36. Kevan, L., and Kispert, L. D. (1976) *Electron spin double resonance spectroscopy*, John Wiley and Sons, New York.
37. Rupp, H., Rao, K. K., Hall, D. O., and Cammack, R. (1978) Electron spin relaxation of iron-sulphur proteins studied by microwave power saturation, *Biochim. Biophys. Acta 537*, 255−260.
38. Hyde, J. S., Rist, G. H., and Eriksson, L. E. G. (1968) Endor of Methyl, Matrix and α Protons in Amorphous and Polycristalline Matrixes, *J. Phys. Chem. 72*, 4269−4277.
39. Lubitz, W., Abresch, E. C., Debus, R. J., Isaacson, R. A., Okamura, M. Y., and Feher, G. (1985) Electron nuclear double resonance of semiquinones in reaction centers of *Rhodopseudomonas sphaeroides*, *Biochim. Biophys. Acta 808*, 464−469.
40. MacMillan, F., Lendzian, F., Renger, G., and Lubitz, W. (1995) EPR and ENDOR investigation of the primary electron acceptor radical anion Q_A^- in iron-depleted photosystem II membrane fragments, *Biochemistry 34*, 8144−8156.
41. Rigby, S. E., Evans, M. C., and Heathcote, P. (1996) ENDOR and special triple resonance spectroscopy of A_1^- of photosystem 1, *Biochemistry 35*, 6651−6656.
42. Salerno, J. C., Osgood, M., Liu, Y. J., Taylor, H., and Scholes, C. P. (1990) Electron nuclear double resonance (ENDOR) of the Qc^- ubisemiquinone radical in the mitochondrial electron transport chain, *Biochemistry 29*, 6987−6993.
43. McCurley, J. P., Miki, T., Yu, L., and Yu, C. A. (1990) EPR characterization of the cytochrome $b-c_1$ complex from *Rhodobacter sphaeroides*, *Biochim. Biophys. Acta 1020*, 176−186.
44. Meinhardt, S. W., and Ohnishi, T. (1992) Determination of the position of the Q_i^- quinone binding site from the protein surface of the cytochrome bc_1 complex in *Rhodobacter capsulates* chromatophores, *Biochim. Biophys. Acta 1100*, 67−74.
45. T'Sai, A. L., and Palmer, G. (1983) Potentiometric studies on yeast complex III, *Biochim. Biophys. Acta 722*, 349−363.
46. Yu, C. A., Nagaoka, S., Yu, L., and King, T. E. (1978) Evidence for the existence of a ubiquinone protein and its radical in the cytochromes *b* and c_1 region in the mitochondrial electron transport chain, *Biochem. Biophys. Res. Commun. 82*, 1070−1078.
47. Burbaev, D. S., Moroz, I. A., Kotlyar, A. B., Sled, V. D., and Vinogradov, A. D. (1989) Ubisemiquinone in the NADH-ubiquinone reductase region of the mitochondrial respiratory chain, *FEBS Lett. 254*, 47−51.
48. Vinogradov, A. D., Sled, V. D., Burbaev, D. S., Grivennikova, V. G., Moroz, I. A., and Ohnishi, T. (1995) Energy-dependent Complex I-associated ubisemiquinones in submitochondrial particles, *FEBS Lett. 370*, 83−87.
49. O'Malley, P. J., and Babcock, G. T. (1984) Elucidation of the principal hyperfine tensor components for the methyl group interaction in semiquinone anion radicals utilizing powder ENDOR spectroscopy, *J. Phys. Chem. 80*, 3912−3913.
50. Feher, G., Isaacson, R. A., Okamura, M. Y., and Lubitz, W. (1985) ENDOR of semiquinones in RCs from *Rhodopseudomonas sphaeroides*, in *Antennas and Reaction Centers of Photosynthetic Bacteria* (Michel-Beyerle, M. E., Ed.) pp 174−189, Springer-Verlag, Berlin and Heidelberg.
51. Grimaldi, S. (2002) Multidimensional electron paramagnetic resonance spectroscopy on protein bound semiquinones, Doctoral Thesis, J.-W. Goethe Universität, Frankfurt, Germany.
52. Dorlet, P., Rutherford, A. W., and Un, S. (2000) Orientation of the tyrosyl D, pheophytin anion, and semiquinone Q_A^- radicals in photosystem II determined by high-field electron paramagnetic resonance, *Biochemistry 39*, 7826−7834.

53. Burghaus, O., Plato, M., Rohrer, M., Möbius, K., MacMillan, F., and Lubitz, W. (1993) 3-mm high-field EPR on semiquinone radical anions Q^- related to photosynthesis and on the primary donor P^+ and acceptor Q_A^- in reaction centers of *Rhodobacter sphaeroides* R-26, *J. Phys. Chem. 97*, 7639−7647.
54. Isaacson, R. A., Lendzian, F., Abresch, E. C., Lubitz, W., and Feher, G. (1995) Electronic structure of Q^-_A in reaction centers from *Rhodobacter sphaeroides*. I. Electron paramagnetic resonance in single crystals, *Biophys. J. 69*, 311−322.
55. Un, S., Dorlet, P., and Rutherford, A. W. (2001) A high-field EPR tour of radicals in photosystems I and II, *Appl. Magn. Reson. 21*.
56. MacMillan, F., Hanley, J., van der Weerd, L., Knupling, M., Un, S., and Rutherford, A. W. (1997) Orientation of the phylloquinone electron acceptor anion radical in photosystem I, *Biochemistry 36*, 9297−9303.
57. Gardiner, A. T., Zech, S. G., MacMillan, F., Kass, H., Bittl, R., Schlodder, E., Lendzian, F., and Lubitz, W. (1999) Electron paramagnetic resonance studies of zinc-substituted reaction centers from *Rhodopseudomonas viridis*, *Biochemistry 38*, 11773−11787.

BI048009R